Environmental Science
Processes & Impacts

PAPER

View Article Online
View Journal | View Issue

Open Access Article. Published on 07 dezembro 2015. Downloaded on 17/11/2024 04:07:55.
This article is licensed under a Creative Commons Attribution 3.0 Unported Licence.

Cite this: *Environ. Sci.: Processes Impacts*, 2016, **18**, 208

Assessment of the long-term impacts of PM_{10} and $PM_{2.5}$ particles from construction works on surrounding areas†

Farhad Azarmi,[a] Prashant Kumar,*[ab] Daniel Marsh[c] and Gary Fuller[c]

Received 21st October 2015
Accepted 3rd December 2015

DOI: 10.1039/c5em00549c

rsc.li/process-impacts

Construction activities are common across cities; however, the studies assessing their contribution to airborne PM_{10} (≤10 μm) and $PM_{2.5}$ (≤2.5 μm) particles on the surrounding air quality are limited. Herein, we assessed the impact of PM_{10} and $PM_{2.5}$ arising from construction works in and around London. Measurements were carried out at 17 different monitoring stations around three construction sites between January 2002 and December 2013. Tapered element oscillating microbalance (TEOM 1400) and OSIRIS (2315) particle monitors were used to measure the PM_{10} and $PM_{2.5}$ fractions in the 0.1–10 μm size range along with the ambient meteorological data. The data was analysed using bivariate concentration polar plots and *k*-means clustering techniques. Daily mean concentrations of PM_{10} were found to exceed the European Union target limit value of 50 μg m^{-3} at 11 monitoring stations but remained within the allowable 35 exceedences per year, except at two monitoring stations. In general, construction works were found to influence the downwind concentrations of PM_{10} relatively more than $PM_{2.5}$. Splitting of the data between working (0800–1800 h; local time) and non-working (1800–0800 h) periods showed about 2.2-fold higher concentrations of PM_{10} during working hours when compared with non-working hours. However, these observations did not allow to conclude that this increase was from the construction site emissions. Together, the polar concentration plots and the *k*-means cluster analysis applied to a pair of monitoring stations across the construction sites (*i.e.* one in upwind and the other in downwind) confirmed the contribution of construction sources on the measured concentrations. Furthermore, pairing the monitoring stations downwind of the construction sites showed a logarithmic decrease (with R^2 about 0.9) in the PM_{10} and $PM_{2.5}$ concentration with distance. Our findings clearly indicate an impact of construction activities on the nearby downwind areas and a need for developing mitigation measures to limit their escape from the construction sites.

Environmental impact

Construction activities have potential to increase the local concentrations of coarse and fine particles, which adversely affect public health. Increased construction activities are expected to cope with the growing world population, which highlights the importance of particle emissions from these sources. This study assesses the impact of PM_{10} (≤10 μm) and $PM_{2.5}$ (≤2.5 μm) arising from outdoor construction works on the surrounding environment in London. Increased concentrations at monitoring stations downwind of the construction sites suggest a need to develop efficient mitigation strategies to limit the escape of particulate matter from construction sites.

1. Introduction

Construction developments in both the developing and developed world are common. However, the impact of particulate matter (PM) emitted in the coarse ($PM_{2.5–10}$; between 2.5 and 10 μm) and fine ($PM_{2.5}$ ≤ 2.5 μm) particle size range from such activities on the surrounding areas is poorly understood. Construction and demolition of structures is known to result in higher local concentrations of PM_{10}, which contains a wide variety of toxic organic substances and may adversely affect the respiratory health of nearby residents.[1–5] There is also an increased interest in $PM_{2.5}$ because it penetrates deeper into the

[a]*Department of Civil and Environmental Engineering, Faculty of Engineering and Physical Sciences, University of Surrey, Guildford GU2 7XH, UK. E-mail: P.Kumar@surrey.ac.uk; Prashant.Kumar@cantab.net; Fax: +44 (0)1483 682135; Tel: +44 (0) 1483 682762*

[b]*Environmental Flow (EnFlo) Research Centre, Faculty of Engineering and Physical Sciences, University of Surrey, Guildford GU2 7XH, UK*

[c]*MRC PHE Centre for Environment and Health, King's College London, London SE1 9NH, UK*

† Electronic supplementary information (ESI) available: Sections S1–S2, Tables S1–S4 and Fig. S1–S5. See DOI: 10.1039/c5em00549c

This journal is © The Royal Society of Chemistry 2016

Open Access Article. Published on 07 dezembro 2015. Downloaded on 17/11/2024 04:07:55.
This article is licensed under a Creative Commons Attribution 3.0 Unported Licence.

lungs and is of even greater concern for human health.[6–8] For this reason, exposure to $PM_{2.5}$ is globally the 9th most powerful risk factor for disease burden.[9,10] Until recently, only limited study has focused on the exposure to PM_{10} and even less research on exposure to $PM_{2.5}$ fractions arising from outdoor construction activities and understanding their potential impact on local air quality (Table 1).

Besides construction activities, PM_{10} concentrations are also affected by the emissions arising from local fugitive sources such as road works,[11–15] vehicle exhaust[16–20] and non-vehicle exhaust sources.[21–26] At the same time, many activities associated with air and sea transportation produce particles across the range of PM_{10} and $PM_{2.5}$.[27–29] A few studies have investigated the PM_{10} emissions arising from industrial sources such as waste transfer stations.[30] There are also a few studies concerned with PM_{10} emissions arising from outdoor construction activities.[31–35] However, there is still very little work focused on $PM_{2.5}$ fractions arising from construction activities.[36]

The importance of particle exposure from construction sources is expected to increase with the ever growing world population.[37,38] In addition to concerns associated with the short-term exposure to airborne PM at the time of construction activities, there is also the potential for long-term exposure to PM that settles across the nearby community, which is then available for inhalation or ingestion after resuspension.[32,39,40]

The European Union[41] set the targets to limit the daily and annual mean values of PM_{10} at a European-wide level for the years 2004 and 2010.[13] The legal limit by 2005 was to achieve a daily mean PM_{10} concentration of 50 $\mu g\ m^{-3}$, not exceeded on more than 35 occasions per year and annual mean values of 40 $\mu g\ m^{-3}$. Moreover, the target by 2010 was to achieve a daily mean PM_{10} concentration of 50 $\mu g\ m^{-3}$, not exceeded on more than 7 occasions per year and annual mean concentrations of 20 $\mu g\ m^{-3}$. These target values, to be met by 2010, were not carried forward in Directive 2008/50/EC.[42] Fuller and Green[13] noted that the PM_{10} emissions generated by building and road works in and around London breached the EU limits for the daily mean PM_{10} concentrations (50 $\mu g\ m^{-3}$) on several occasions. In this study, a series of PM_{10} and $PM_{2.5}$ measurements at 17 monitoring stations around construction sites were carried out during 2002–2013 to assess their impact on the air quality in the surrounding areas.

2. Materials and methods

2.1 Description of the construction sites

Measurements were carried out around three outdoor construction sites, which are referred hereafter as CS_1, CS_2 and CS_3. CS_1, CS_2 and CS_3 covered an area of about 260×10^4, 54×10^4 and 3×10^4 m^2, respectively (Fig. 1). There were 17 monitoring stations (*i.e.* MS_1–MS_{17}) around these three outdoor construction sites (CS_1, CS_2 and CS_3), which represent a diverse range of construction activities. The locations of the monitoring stations around these sites are shown in Fig. 1, but the specific details about the location have been kept anonymous for the protection of confidential information.

2.2 Field measurements

Continuous air quality monitoring was carried out at 17 different monitoring stations around three construction sites to measure the concentration of PM_{10} and $PM_{2.5}$. The measurements of PM concentrations analysed in this study were during the periods of construction and there were no similar measurements made before and/or after the construction works. Measurements were undertaken continuously and divided into working hours (referred to as working period) in weekdays between 08:00 and 18:00 h (local time) and non-working hours (referred to as non-working period), which covered the weekdays between 18:00 and 08:00 h and the weekends. Data were collected over a period of about 4000 days for about 12 years between 2002 and 2013 at the 17 different monitoring sites around CS_1–CS_3 (Table 2). A diverse range of

Table 1 A summary of the past studies showing the measured PM concentrations from various outdoor building activities

Activity type	Pollutant type	Characteristics	Reference
Building and road works	PM_{10}	Outdoor (at over 80 monitoring sites in and around London, UK)	Fuller and Green[13]
Building implosion	PM_{10}	Outdoor (22-story building in east Baltimore, USA)	Beck *et al.*[32]
Building demolition	PM_{10}	Outdoor (three public housing developments in Chicago, USA)	Dorevitch *et al.*[33]
Building demolition	PM_{10}	Outdoor (demolition of an old four-story building on the premises of the University Hospital of Essen, Germany)	Hansen *et al.*[31]
Construction activities	PM_{10}	Outdoor (construction and operational activities at a port in Mumbai, India)	Joseph *et al.*[34]
Earthmoving activities	PM_{10} and $PM_{2.5}$	Outdoor (earth moving activities conducted at two Kansas sites, Kansas city, USA)	Muleski *et al.*[36]
Road widening and construction activities	PM_{10} and $PM_{2.5}$	Outdoor (road widening and related construction works in London, UK)	Font *et al.*[57]

Open Access Article. Published on 07 dezembro 2015. Downloaded on 17/11/2024 04:07:55.
This article is licensed under a Creative Commons Attribution 3.0 Unported Licence.

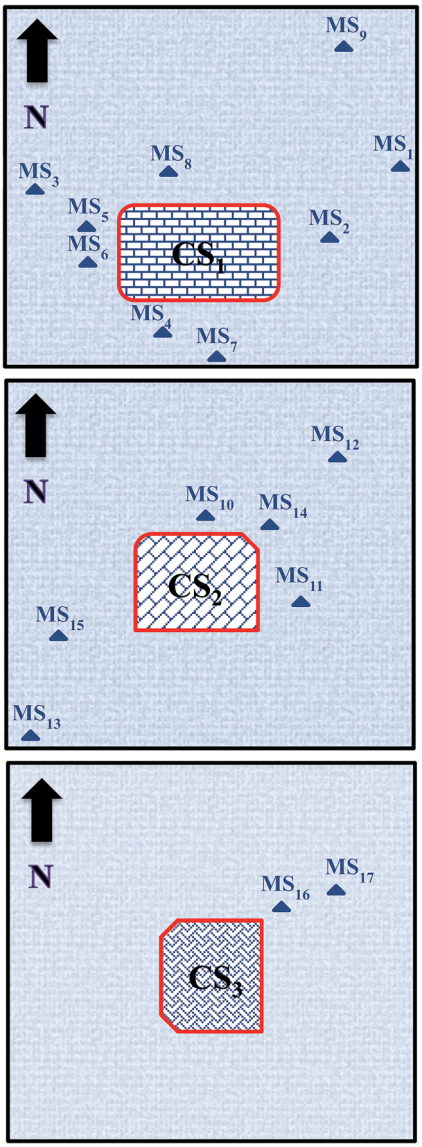

Fig. 1 Schematic of the experimental set-up showing the monitoring stations (MS) and construction sites (CS). Please note that the figure is not to scale and the distances are presented in Table 2.

construction works during the different phases of the construction were anticipated at the studied sites. However, we did not have access to information of the different phases of the construction processes at each site, except the overall duration of the works.

Data were analysed with reference to the EU Limit Values for annual and daily PM_{10} concentrations. In addition, bivariate plots were drawn to qualitatively assess the effects of wind speed and direction on the measured concentrations in upwind and downwind directions from construction sites. The *k*-means clustering technique was then applied to assess contribution of probable local construction sources, which were identified through bivariate polar plots of paired monitoring stations (*i.e.* one in upwind and the other in downwind). The *k*-means clustering technique helped to identify the range of increases in particle mass concentrations due to the construction operations, including the resuspension and emissions from any on-site vehicles.[43] Moreover, the frequency and variation in PM_{10} and $PM_{2.5}$ concentration in the prevailing wind direction were evaluated with changes in distance from sources by pairing the sites in downwind of the CS_1–CS_3 to assess the decay profile of the PM emissions, which is important to understand the impact of the construction works on the air quality in surrounding areas.

2.3 Instrumentation

PM concentrations at CS_1 were collected using a Tapered Element Oscillating Monitor (TEOM 1400) and those at CS_2 and CS_3 were measured using a Turnkey Osiris instrument (model 2315). Practical constraints, such as space and cost, were important factors in the instrument selection.

The TEOM 1400 was used to measure mass of particles per unit volume of air in the size range of 0.1–10 μm. The sampling stream and filters were heated to 50 °C to maintain a stable temperature and to eliminate interference from water on the filter.[44] The mass measurement relied on the measurement of the resonant frequency of an oscillating system that consists of the filter and glass element. A correction factor of 1.3 was recommended in the UK for comparison of PM_{10} measurements from TEOM with the EU Directive 1999/30/EC[13,41] prior to the development of a dynamic correction system[45,46] and was applied in this study. Further details about the working principle and sensitivity of the TEOM 1400 can be found elsewhere.[47–49]

The Turnkey Osiris instrument (model 2315) was used to measure the mass distribution of particles per unit volume of air in the 0.4–20 μm size range by light scattering technology in a mass concentration range of 0.1–6000 μg m^{-3}.[50] The Osiris instrument is a portable device that is capable of sampling and measuring particle concentrations in real-time with a high temporal resolution (1 s minimum). The air sample is continuously drawn into the instrument by a pump with a flow rate set by the microprocessor at a rate of 0.6 l min^{-1} through an inlet heated to 50 °C to minimise the effects of water droplets and particle bound water. Over 20 000 particles per second can be sized before coincidence effects occur. Several size selective inlets are also available for the instrument. These can be used to collect a size selected gravimetric sample on the instrument's filter and will measure in μg m^{-3}. The Osiris instrument also allows wind speed and direction, temperature and relative humidity to be recorded at the same time. The Turnkey Instruments, OSIRIS monitors, have also been used for the assessment of indoor and outdoor PM levels as well as personal exposure in a number of past studies.[51,52]

Meteorological data was produced taking a mean from a number of different monitoring locations across the monitoring stations and construction areas wherein the meteorological equipment is considered to be working well and the data shows a good correlation. The measurements were carried out using cup anemometers and wind vanes (as opposed to sonic anemometers) mainly made by Campbell Scientific. This equipment was located at a height of about 10 m.

 This journal is © The Royal Society of Chemistry 2016

Open Access Article. Published on 07 dezembro 2015. Downloaded on 17/11/2024 04:07:55.
This article is licensed under a Creative Commons Attribution 3.0 Unported Licence.

Table 2 A description of the monitoring stations around the construction sites. Monitoring stations MS_1-MS_9, MS_{10}-MS_{15} and MS_{16}-MS_{17} below are around the CS_1, CS_2 and CS_3 sites, respectively

Site code	Duration	Species monitored	Instrument used	Location (distance of the MS from CS)
MS_1	January 2002–January 2007	PM_{10}	TEOM 1400	CS_1 (3000 m)
MS_2	January 2002–January 2007	PM_{10}	TEOM 1400	CS_1 (500 m)
MS_3	January 2002–January 2007	PM_{10}	TEOM 1400	CS_1 (500 m)
MS_4	January 2002–January 2007	PM_{10}, $PM_{2.5}$	TEOM 1400	CS_1 (100 m)
MS_5	January 2002–January 2007	PM_{10}, $PM_{2.5}$	TEOM 1400	CS_1 (200 m)
MS_6	January 2002–January 2007	PM_{10}, $PM_{2.5}$	TEOM 1400	CS_1 (200 m)
MS_7	January 2002–January 2007	PM_{10}, $PM_{2.5}$	TEOM 1400	CS_1 (500 m)
MS_8	January 2002–January 2007	PM_{10}, $PM_{2.5}$	TEOM 1400	CS_1 (500 m)
MS_9	January 2002–January 2007	PM_{10}, $PM_{2.5}$	TEOM 1400	CS_1 (4000 m)
MS_{10}	January 2009–December 2013	PM_{10}	OSIRIS 2315	CS_2 (100 m)
MS_{11}	December 2009–May 2013	PM_{10}	OSIRIS 2315	CS_2 (200 m)
MS_{12}	November 2008–December 2013	PM_{10}	OSIRIS 2315	CS_2 (1000 m)
MS_{13}	January 2009–December 2013	PM_{10}	OSIRIS 2315	CS_2 (3000 m)
MS_{14}	May 2013–December 2013	PM_{10}	OSIRIS 2315	CS_2 (100 m)
MS_{15}	January 2009–October 2014	PM_{10}	OSIRIS 2315	CS_2 (400 m)
MS_{16}	June 2011–August 2012	PM_{10}	OSIRIS 2315	CS_3 (100 m)
MS_{17}	June 2011–August 2012	PM_{10}	OSIRIS 2315	CS_3 (50 m)

3. Results and discussion

3.1 Bivariate concentration polar plots

Fig. 2 shows the polar plots that were constructed by partitioning wind speed and direction data and their corresponding hourly mean PM concentration data into different wind speed and direction bins.[43] These plots are presented as smoothed surfaces showing the variations in concentration, depending on the local wind direction and wind speed at a receptor.[53] The results presented in Fig. 2 show evidence of increased concentrations levels of PM_{10} and $PM_{2.5}$ when the wind direction was from the construction sites to the monitoring stations.

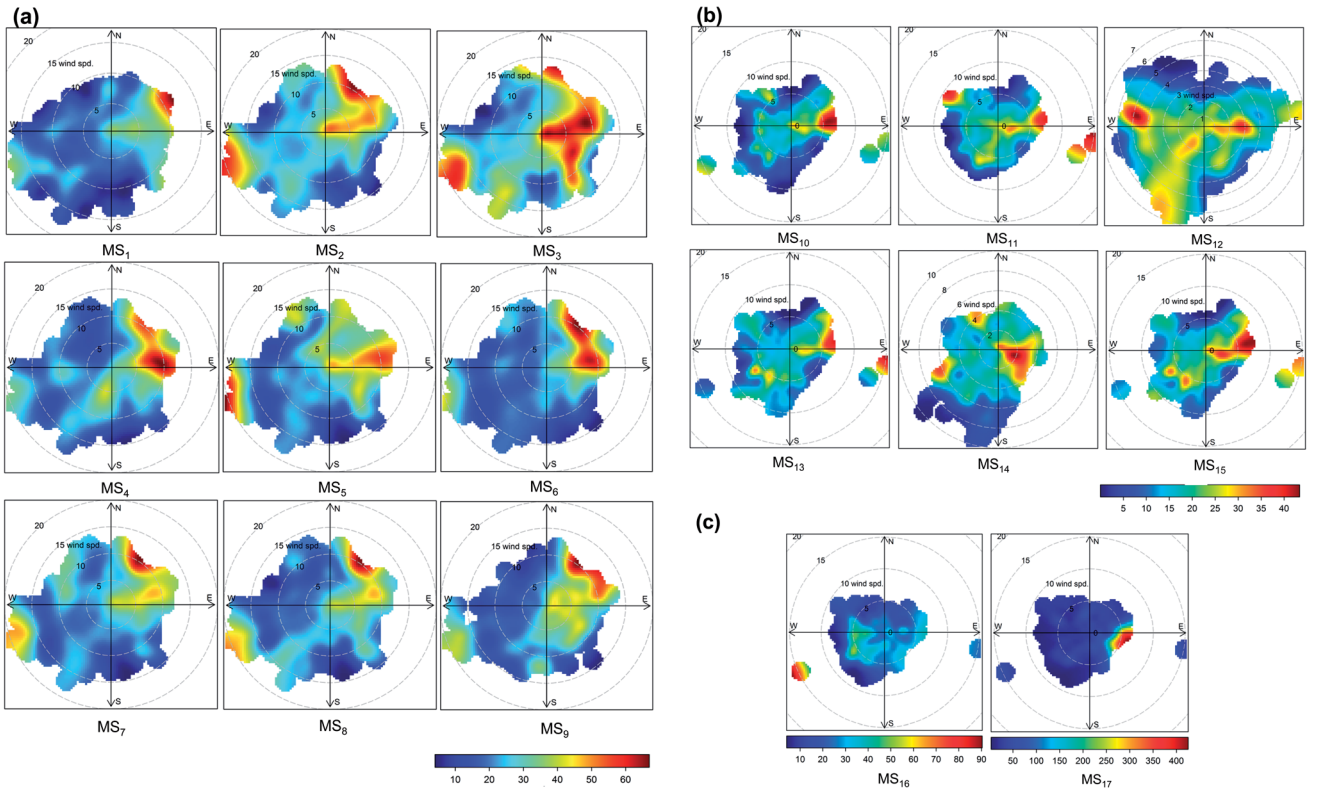

Fig. 2 Polar plots for PM_{10} at (a) CS_1, (b) CS_2 and (c) CS_3; hourly average values were used for all pollutants. These plots are presented as smoothed surfaces showing how the concentrations vary depending on the local wind speed and wind direction.

Open Access Article. Published on 07 dezembro 2015. Downloaded on 17/11/2024 04:07:55.
This article is licensed under a Creative Commons Attribution 3.0 Unported Licence.

Closer inspection of polar plots at all 17 monitoring stations around each of the three sites indicates the following: first, whenever there are monitoring stations in the downwind side of the construction sites, high concentrations of PM_{10} (Fig. 2) and $PM_{2.5}$ (Fig. 3) are observed, indicating a potential contribution from the construction activities (Fig. 2). Second, pockets of high PM concentrations can also be observed in some cases (for example, observe MS_2 for PM_{10} and MS_9 for $PM_{2.5}$ in Fig. 2a and 3, respectively) despite the monitoring stations being in the upwind of the east and south-west wind directions. This was expected due to long-range transport of PM_{10} during easterly winds from European countries[54,55] and the effect of generated sea salt on $PM_{2.5}$ from the south-westerly winds.[55,56] This observation also suggests that the concentrations measured downwind of the construction sites include some contribution of emissions from these sources and are not solely from the emissions of the construction activities. However, this analysis was inadequate to conclusively report that the measured downwind emissions are from the construction sites. Therefore, paired-site (Section 3.2) and *k*-means (Section 3.3) analyses were performed to better understand the contributions of the construction emissions during varying wind directions.

3.2 Assessment of the paired sites for examining differences in PM concentrations

We paired the monitoring stations opposite to each other, upwind and downwind of the construction sites to assess the relative changes in the concentrations that may have been contributed by the construction emissions (Fig. 4). We found two pairs of paired monitoring stations each for PM_{10} and $PM_{2.5}$ around CS_1 (Fig. 4a) and another two pairs for PM_{10} around CS_2 (Fig. 4b), giving a total of 6 paired monitoring stations. This pairing allowed us to measure changes in the concentrations (*i.e.* ΔPM_{10} and $\Delta PM_{2.5}$) as air mass crosses the construction sites and the results are presented in Fig. 4. For example, the hourly mean differences in PM_{10} and $PM_{2.5}$ at CS_1 measured in the two pairs of opposite monitoring stations (MS_1, MS_4 and MS_7, MS_8), which were estimated as MS_4 minus MS_1 and MS_7 minus MS_8. Likewise, the hourly mean differences at CS_2 were calculated using MS_{14} and MS_{15} as opposite monitoring stations, which was MS_{15} minus MS_{14}. Subtraction of the results in the upwind polar plots from those in downwind polar plots clearly shows an increase in the concentrations of PM_{10} and $PM_{2.5}$ at all the sites, with all the values being positive and high concentration zone reflecting emissions from the construction sites. Cross-comparison of results between different PM types

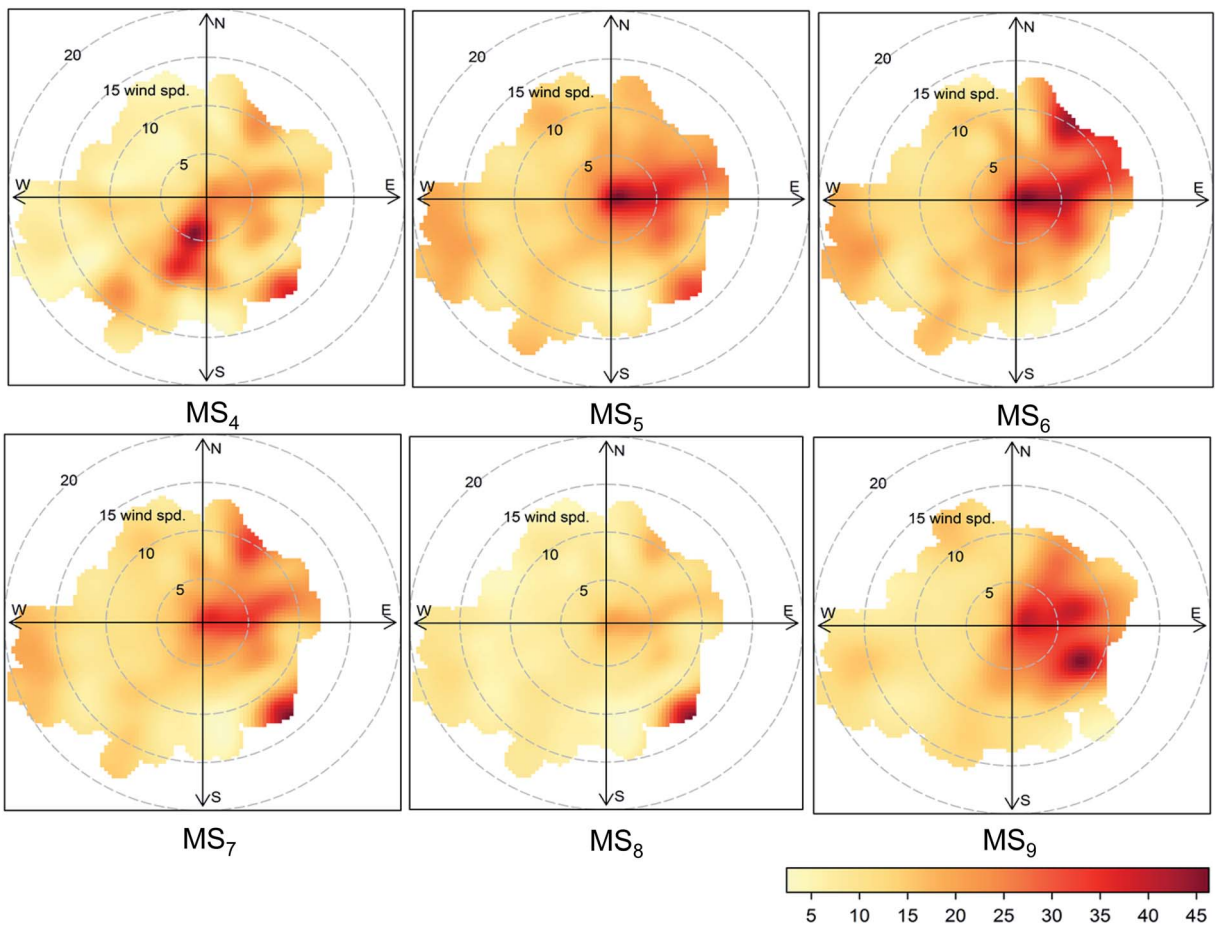

Fig. 3 Polar plots for $PM_{2.5}$ (hourly average values were used for all pollutants) at CS_1. These plots are presented as smoothed surfaces showing how the concentrations vary depending on the local wind speed and wind direction.

 This journal is © The Royal Society of Chemistry 2016

Open Access Article. Published on 07 dezembro 2015. Downloaded on 17/11/2024 04:07:55.
This article is licensed under a Creative Commons Attribution 3.0 Unported Licence.

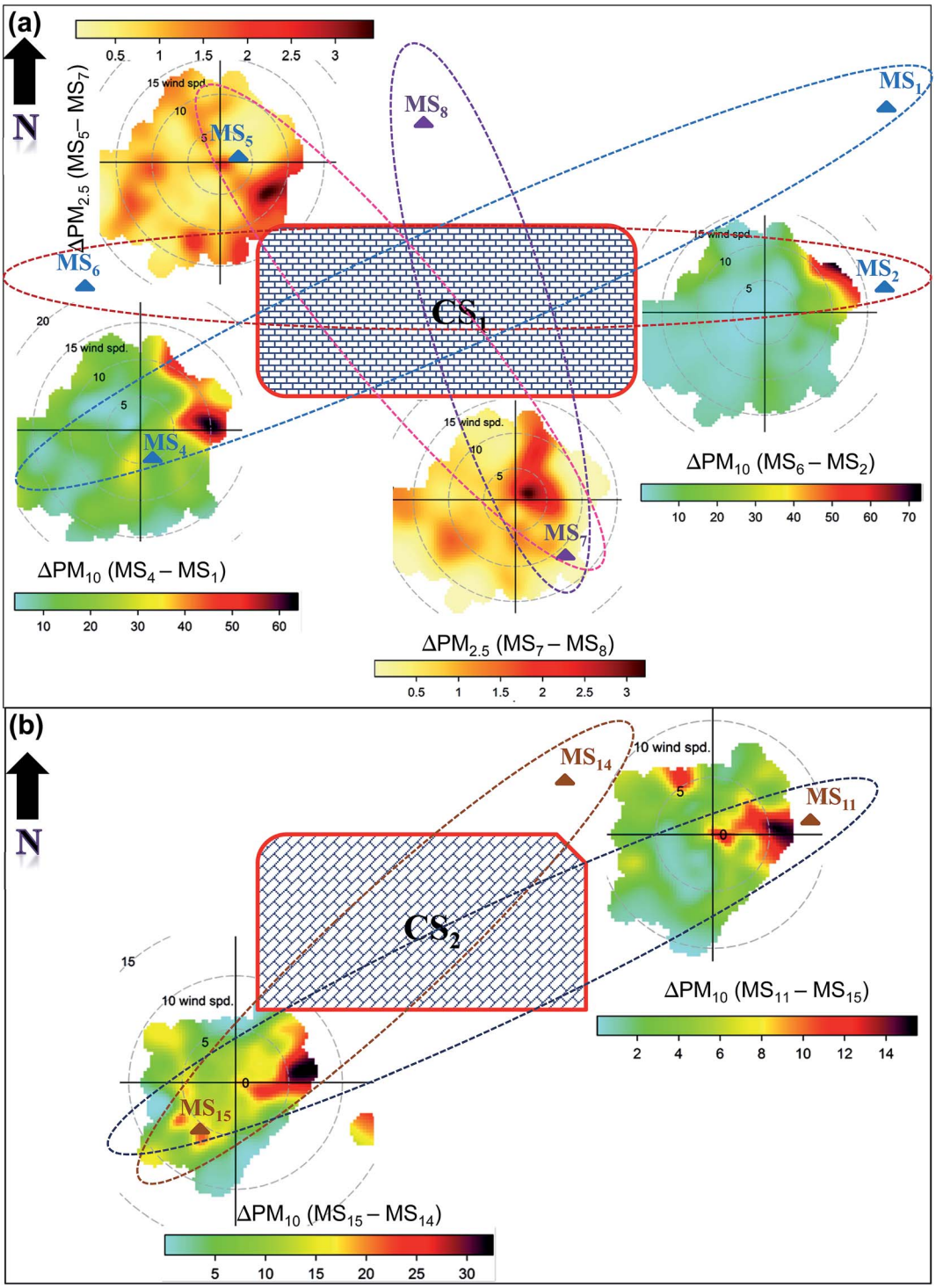

Fig. 4 The polar plots for the paired monitoring stations across each construction site, for ΔPM_{10} and $\Delta PM_{2.5}$ (a) at CS_1 and (b) for ΔPM_{10} at CS_2, respectively. These plots are presented as smoothed surfaces, showing that the concentrations vary depending on the local wind speed and wind direction.

suggest that the differences are larger for PM_{10} when compared with $PM_{2.5}$, suggesting a relatively greater variability in PM_{10} emissions than those in $PM_{2.5}$ from construction works. Similar observations were reported by previous studies[57] wherein they found greater increases in PM_{10} compared with $PM_{2.5}$ from road widening works in London.

3.3 *k*-Means cluster analysis

To identify and independently assess the contribution from local sources, *k*-means cluster analysis was applied on the 6 paired monitoring stations that were identified and discussed in Section 3.2. Eight different clusters were chosen that were

Open Access Article. Published on 07 dezembro 2015. Downloaded on 17/11/2024 04:07:55.
This article is licensed under a Creative Commons Attribution 3.0 Unported Licence.

found to be optimal for separating the local source contribution from external sources, based on the recommendations from previous studies.[53,58–60]

Fig. 5 and 6 show the contribution of each cluster in the polar plots of ΔPM_{10} and $\Delta PM_{2.5}$. The temporal variation of ΔPM_{10} and $\Delta PM_{2.5}$ contributed by each cluster on an hourly, weekly and monthly basis are also shown. Based on the ΔPM_{10} and $\Delta PM_{2.5}$ concentrations showing the high concentration peaks in the polar plots (Fig. 4), clusters 5–7 can be identified to represent the concentrations of ΔPM_{10} (Fig. 5) and $\Delta PM_{2.5}$ (Fig. 6) due to construction sources. If we observe these clusters in the temporal variation plots, peaks can be observed during the weekdays, which are missing during the weekends. This is also demonstrated by the increases in the PM_{10} and $PM_{2.5}$ concentrations during 08:00 and 18:00 h, which we referred to as "working hours". The temporal plots on a monthly basis were examined and the identified clusters (*i.e.* 5–7) showed relatively lower concentrations during the cold months (*i.e.* December, January and February) compared with the rest of the months. There could be two possible reasons for these lower concentrations: (i) less construction activity compared to normal and (ii) the weather conditions suppressing the emissions and transport of particles due to relatively wetter conditions than the other months and also affecting the normal construction due to adverse weather conditions. For example, the mean precipitation and relative humidity is expected to be higher during winter months (*e.g.* 256 mm and 85% to 213 mm and 70% during summer) and low temperature (*e.g.* mean ~4 °C to 15 °C during summer).[61] Past studies have found wet conditions such as water spraying an effective method to suppress coarse particle emissions by up to 13-times during construction works.[62] Detailed receptor modelling studies could help further in drawing firm conclusions.

3.4 Particle mass concentrations during working and non-working hours

Fig. 7 shows the annual mean PM_{10} and $PM_{2.5}$ concentrations at the three construction sites. The annual average in PM_{10} concentrations were found to be 22.9 ± 3.3 μg m^{-3}, 18.8 ± 2.2 μg m^{-3} and 34.9 ± 2.8 μg m^{-3} at CS_1 (Table 3), CS_2 (Table 5) and CS_3 (Table 6), respectively, whereas the annual average $PM_{2.5}$ concentrations were 14.0 ± 1.7 μg m^{-3} at CS_1 (Table 4). These averages include both the working and non-working hours and the averages for these separate durations are presented in ESI Fig. S1a and S2 and described in ESI Sections S1–S2.† Depending on the source and distance from the monitoring stations, the values of PM_{10} and $PM_{2.5}$ varied and the concentrations in all cases increased as the working period started (ESI Fig. S1–S4†).

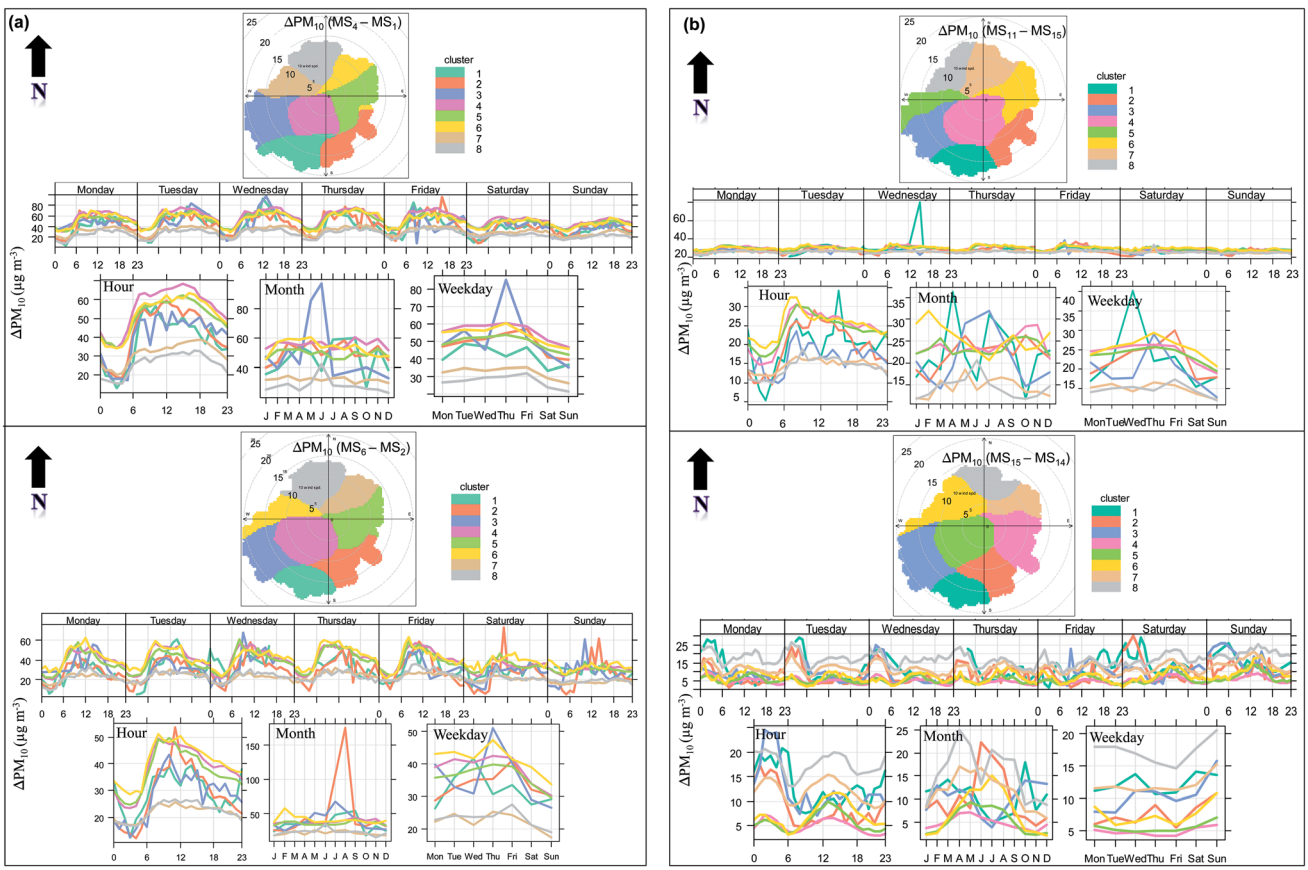

Fig. 5 Clusters identified at the CS_1 and CS_2 sites for PM_{10} concentrations for 8 clusters. The shading shows the 95% confidence intervals in the mean. The data have been normalised in each case by dividing by the mean.

 This journal is © The Royal Society of Chemistry 2016

Open Access Article. Published on 07 dezembro 2015. Downloaded on 17/11/2024 04:07:55.
This article is licensed under a Creative Commons Attribution 3.0 Unported Licence.

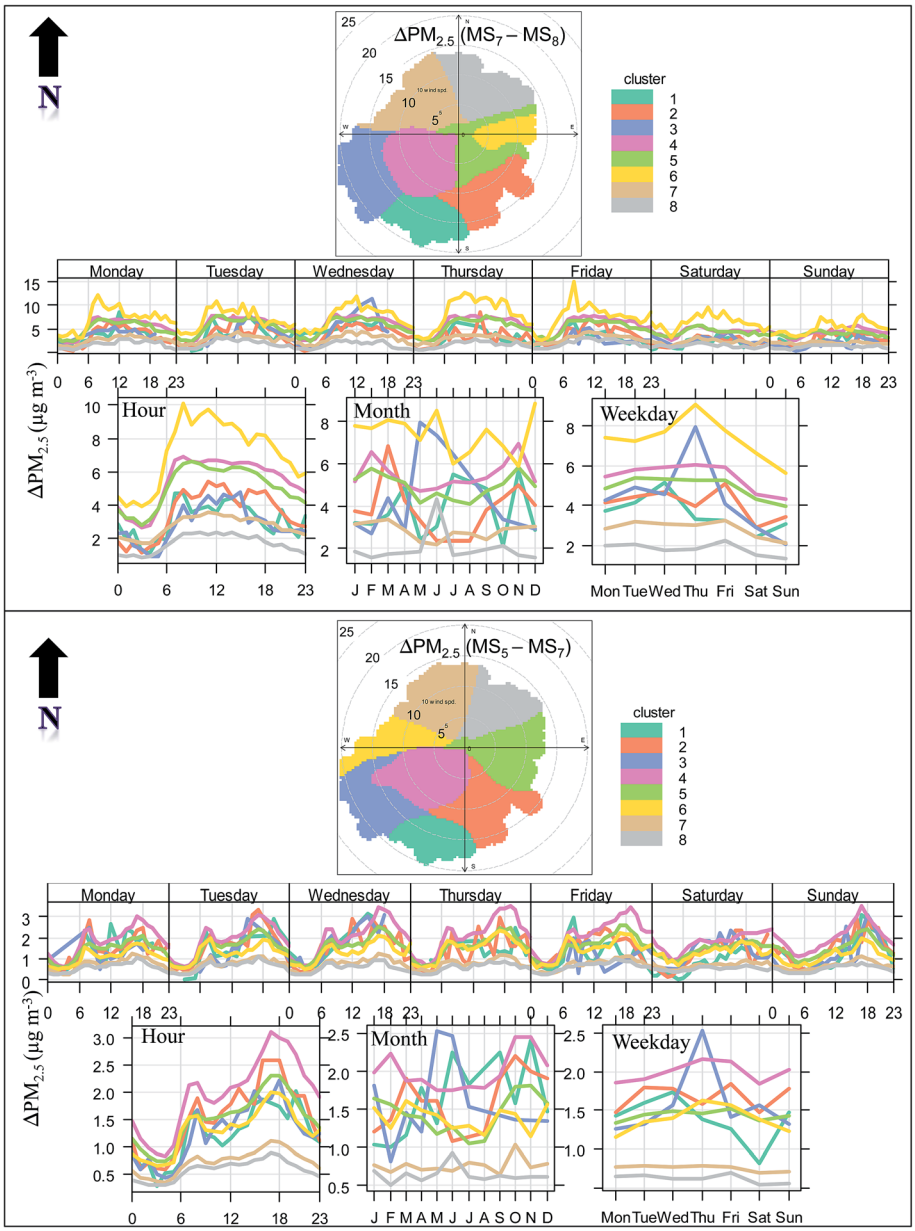

Fig. 6 Clusters identified at CS_1 for $PM_{2.5}$ concentrations for 8 clusters. The shading shows the 95% confidence intervals in the mean. The data have been normalised in each case by dividing by the mean.

In general, the concentrations observed during the working hours were higher than those during non-working hours (ESI Tables S1–S4†), presumably due to construction activities and the other emission sources such as road vehicles in operation during working hours. Moreover, exhaust and non-exhaust construction sources were at rest during the non-working hours and therefore these are unlikely to contribute to the observed variations during the night. Because there was no major roadway around CS_1, the variation in particle mass concentrations (PMCs) between the three construction sites during working and non-working hours could be attributed to the variability in meteorological conditions (mainly wind speed and direction; Fig. 2 and 3) during the different years of the measurements. Overall, the PM_{10} values were about ~24%, 18% and 120% larger during the working periods when compared with those observed during the non-working periods at CS_1, CS_2 and CS_3, respectively. Moreover, at CS_1, there was an increase of about 11% in $PM_{2.5}$ values during the working period when compared with the non-working periods (ESI Fig. S2†).

A comparison of the 24 hour average concentrations of PM_{10} with the EU Directive 2008/50/EC,[42] as described in Table 7, suggests the number of exceedences each year (Table 8 and ESI Fig. S5†). However, these exceedences are not expected to be due to construction works alone, given that the winds were blowing from various directions (Fig. 1 and 2) and the presence of nearby sources could also have made a contribution to these exceedences. Therefore, we filtered the data based on the wind direction on an hourly basis at each monitoring station (Fig. 8). The

Open Access Article. Published on 07 dezembro 2015. Downloaded on 17/11/2024 04:07:55.
This article is licensed under a Creative Commons Attribution 3.0 Unported Licence.

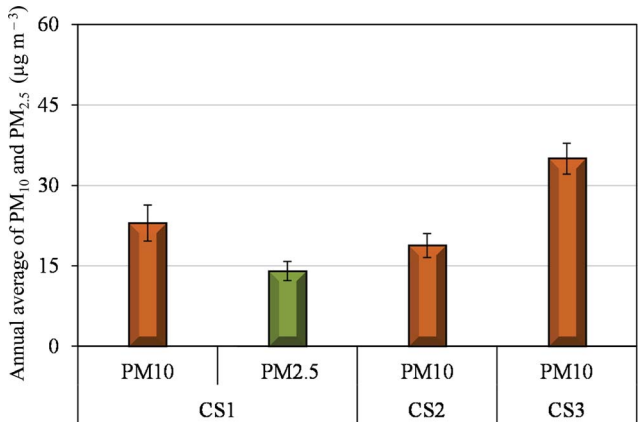

Fig. 7 The annual average concentrations of PM_{10} (17 monitoring stations) during the 2002–2013 period at (a) CS_1, (b) CS_2, and (c) CS_3.

Table 6 The average concentrations of PM_{10}, including the working and non-working periods at CS_3; ± refers to standard deviation

	Monitoring stations	
Year	MS_{16}	MS_{17}
2011	37.3 ± 33.0	35.3 ± 31.2
2012	28.5 ± 24.3	38.6 ± 24.6
Overall average	32.9 ± 19.3	34.9 ± 18.1

monitoring stations downwind of the construction sites were then considered for the comparison with the 24 h mean EU limit value of 50 μg m^{-3} to observe the influence of construction works on the exceedences. The values in the parenthesis in Table 8 shows these exceedences possibly due to the construction activities, which were, except on two occasions in 2003

Table 3 The annual average concentrations of PM_{10}, including the working and non-working periods at CS_1; ± refers to standard deviation and "—" to the unavailability of data

	Monitoring stations								
Year	MS_1	MS_2	MS_3	MS_4	MS_5	MS_6	MS_7	MS_8	MS_9
2002	—	21.9 ± 12.2	19.1 ± 11.2	29.5 ± 22.3	27.5 ± 20.9	23.6 ± 15.6	19.3 ± 10.5	19.4 ± 10.2	24.3 ± 14.4
2003	—	24.5 ± 15.7	21.2 ± 12.9	36.7 ± 32.1	26.8 ± 18.6	31.3 ± 27.9	22.1 ± 14.0	23.8 ± 15.5	22.1 ± 13.7
2004	19.1 ± 11.5	21.2 ± 11.9	17.3 ± 9.5	28.9 ± 23.5	21.8 ± 13.1	25.1 ± 25.5	18.7 ± 11.3	20.5 ± 11.8	25.9 ± 17.0
2005	19.6 ± 10.6	23.9 ± 12.1	17.4 ± 10.9	26.7 ± 21.5	23.2 ± 14.1	23.9 ± 19.4	19.1 ± 10.4	19.6 ± 10.2	—
2006	20.4 ± 11.2	24.5 ± 23.5	18.8 ± 9.8	24.8 ± 18.0	24.5 ± 20.8	22.9 ± 15.5	20.6 ± 10.8	21.2 ± 11.7	—
Overall average	19.9 ± 11.1	23.2 ± 15.1	18.7 ± 10.9	29.3 ± 23.5	24.7 ± 17.5	25.3 ± 20.8	20.0 ± 11.4	20.9 ± 11.9	24.1 ± 9.0

Table 4 The annual average concentrations of $PM_{2.5}$, including the working and non-working periods at CS_1; ± refers to standard deviation and "—" to the unavailability of data

	Monitoring stations								
Year	MS_1	MS_2	MS_3	MS_4	MS_5	MS_6	MS_7	MS_8	MS_9
2002	—	—	—	17.3 ± 17.9	13.0 ± 8.0	12.5 ± 8.0	12.0 ± 8.1	11.8 ± 7.2	12.6 ± 7.9
2003	—	—	—	15.5 ± 13.6	14.5 ± 10.3	14.0 ± 9.9	14.2 ± 10.4	15.5 ± 10.7	17.4 ± 10.1
2004	—	—	—	17.0 ± 18.4	12.6 ± 7.4	11.5 ± 7.9	11.5 ± 7.4	12.1 ± 7.5	19.4 ± 13.3
2005	—	—	—	15.4 ± 16.3	12.9 ± 8.2	11.9 ± 8.2	11.9 ± 7.5	12.0 ± 7.4	—
2006	—	—	—	14.6 ± 12.9	13.0 ± 8.0	12.1 ± 8.0	12.1 ± 7.8	12.9 ± 7.4	—
Overall average	—	—	—	16.0 ± 15.8	13.2 ± 8.4	12.9 ± 8.4	12.4 ± 8.2	12.9 ± 8.0	16.5 ± 6.2

Table 5 The annual average concentrations of PM_{10}, including the working and non-working periods; ± refers to standard deviation and "—" to the unavailability of data

	Monitoring stations					
Year	MS_{10}	MS_{11}	MS_{12}	MS_{13}	MS_{14}	MS_{15}
2009	24.8 ± 15.5	18.2 ± 11.0	19.3 ± 11.6	14.7 ± 7.9	—	15.5 ± 9.2
2010	23.6 ± 16.8	17.2 ± 11.2	—	15.7 ± 13.9	—	14.8 ± 10.3
2011	25.1 ± 18.3	18.7 ± 12.6	—	20.4 ± 11.8	—	20.0 ± 13.2
2012	22.2 ± 16.1	18.6 ± 13.7	—	16.4 ± 9.7	—	18.0 ± 15.4
2013	19.7 ± 12.8	15.6 ± 9.4	—	20.0 ± 11	17.4 ± 12.7	19.1 ± 13.6
Overall average	23.1 ± 16.1	17.7 ± 12.3	19.3 ± 11.6	17.4 ± 11.2	17.4 ± 12.7	17.5 ± 13.1

This journal is © The Royal Society of Chemistry 2016

Open Access Article. Published on 07 dezembro 2015. Downloaded on 17/11/2024 04:07:55.
This article is licensed under a Creative Commons Attribution 3.0 Unported Licence.

Table 7 A summary of the EU air quality limit values and UK government objectives for Air Quality Standards, AQS[13,41,42]

Pollutant	Period of averaging	Limit values	Dates to achieve
EU limit value			
PM_{10}	24 hour mean	50 μg m^{-3} not to be exceeded more than 35 times a year	January 2005
	Calendar year	40 μg m^{-3}	January 2005
	24 hour mean	50 μg m^{-3} not to be exceeded more[a] than 7 times a year (target limit value)	January 2010
	Calendar year	20 μg m^{-3} (target limit value)[a]	January 2010
UK government AQS objective			
PM_{10}	24 hour mean	50 μg m^{-3} not to be exceeded more than 10–14 times a year	January 2010
	Calendar year	23–25 μg m^{-3}	January 2010

[a] The EU Directive 1999/30/EC stipulates that the annual mean values of PM_{10} should be less than 20 μg m^{-3} and should not exceed a mean of greater than 50 μg m^{-3} more than 7 days in a year as per the 2010 target limit values. These target values to be met by 2010 were not carried forward in the Directive 2008/50/EC.[42]

Table 8 The number of exceeded days from the EU standard limit and UK government objective (AQS). Please note that the exceedences presented in the parenthesis against each exceedance number represent the exceedences belonging to the 24 h periods when the wind was blowing from construction to the monitoring stations. This represents the possible exceedences due to construction activities. "—" refers to unavailability of data

Monitoring stations	Monitoring years											
	2002	2003	2004	2005	2006	2007	2008	2009	2010	2011	2012	2013
MS_1	0(0)	0(0)	2(2)	1(1)	0(0)	—	—	—	—	—	—	—
MS_2	3(2)	17(14)	3(1)	2(2)	5(3)	—	—	—	—	—	—	—
MS_3	1(0)	9(7)	0(0)	1(1)	0(0)	—	—	—	—	—	—	—
MS_4	9(6)	60(48)	19(12)	11(7)	5(4)	—	—	—	—	—	—	—
MS_5	18(16)	22(16)	1(0)	6(6)	15(14)	—	—	—	—	—	—	—
MS_6	7(4)	42(36)	16(15)	9(6)	6(6)	—	—	—	—	—	—	—
MS_7	1(0)	11(7)	1(1)	1(1)	1(0)	—	—	—	—	—	—	—
MS_8	0(0)	14(12)	2(0)	1(0)	1(1)	—	—	—	—	—	—	—
MS_9	4(4)	6(5)	3(0)	0(0)	0(0)							
MS_{10}	—	—	—	—	—	—	—	3(1)	17(3)	28(10)	12(12)	6(5)
MS_{11}	—	—	—	—	—	—	—	0(0)	11(7)	31(10)	16(14)	13(13)
MS_{12}	—	—	—	—	—	—	—	0(0)	0(0)	3(3)	5(4)	0(0)
MS_{13}	—	—	—	—	—	—	—	0(0)	0(0)	3(2)	1(1)	0(0)
MS_{14}	—	—	—	—	—	—	—	0(0)	0(0)	0(0)	0(0)	0(0)
MS_{15}	—	—	—	—	—	—	—	0(0)	0(0)	7(5)	6(5)	2(2)
MS_{16}	—	—	—	—	—	—	—	—	—	20(17)	4(4)	—
MS_{17}	—	—	—	—	—	—	—	—	—	25(22)	33(22)	—

(Table 8), less than the allowable 35 exceedences per year (Table 7). Unlike previous studies[13] where the exceedences of daily mean PM_{10} concentrations were reported over the EU limit value of 50 μg m^{-3} on several occasions during the monitoring of emissions from road and building works in London, our exceedences are within the regulatory limits and could also be attributed to the construction works, given that the paired polar roses and *k*-means clusters analysis in Sections 3.1–3.3 suggesting a clear contribution of the construction works on the downwind monitoring stations.

3.5 Decay profiles of PM_{10} and $PM_{2.5}$

The purpose of this section is to evaluate the variation in concentrations of PM_{10} and $PM_{2.5}$ at different distances from the construction sites. This analysis assisted in understanding how far the PM concentrations can go to affect the surrounding areas as well as help in planning for emission mitigation measures, particularly for construction sites close to sensitive areas such as hospitals or schools.

Fig. 9 shows the decay profiles of the PM_{10} and $PM_{2.5}$ concentrations with the changing distance from CS_1 and CS_2. Both the logarithmic (Fig. 9a) and exponential (Fig. 9b) best-fit functions were applied to our ΔPM_{10} and $\Delta PM_{2.5}$. The logarithmic decay function (Fig. 9a) was chosen as a best fit to our data based on better R^2 values than those given by an exponential decay profile as 0.79, 0.90 and 0.89 for PM_{10} (CS_1), PM_{10} (CS_2) and $PM_{2.5}$ (CS_1), respectively (Fig. 9b). The differences between the hourly averages of PM_{10} and $PM_{2.5}$ concentrations (ΔPM_{10} and $\Delta PM_{2.5}$) during the working and non-working time periods provided the net concentrations from the construction activities, which were then used to draw decay profiles (Fig. 9).

Open Access Article. Published on 07 dezembro 2015. Downloaded on 17/11/2024 04:07:55.
This article is licensed under a Creative Commons Attribution 3.0 Unported Licence.

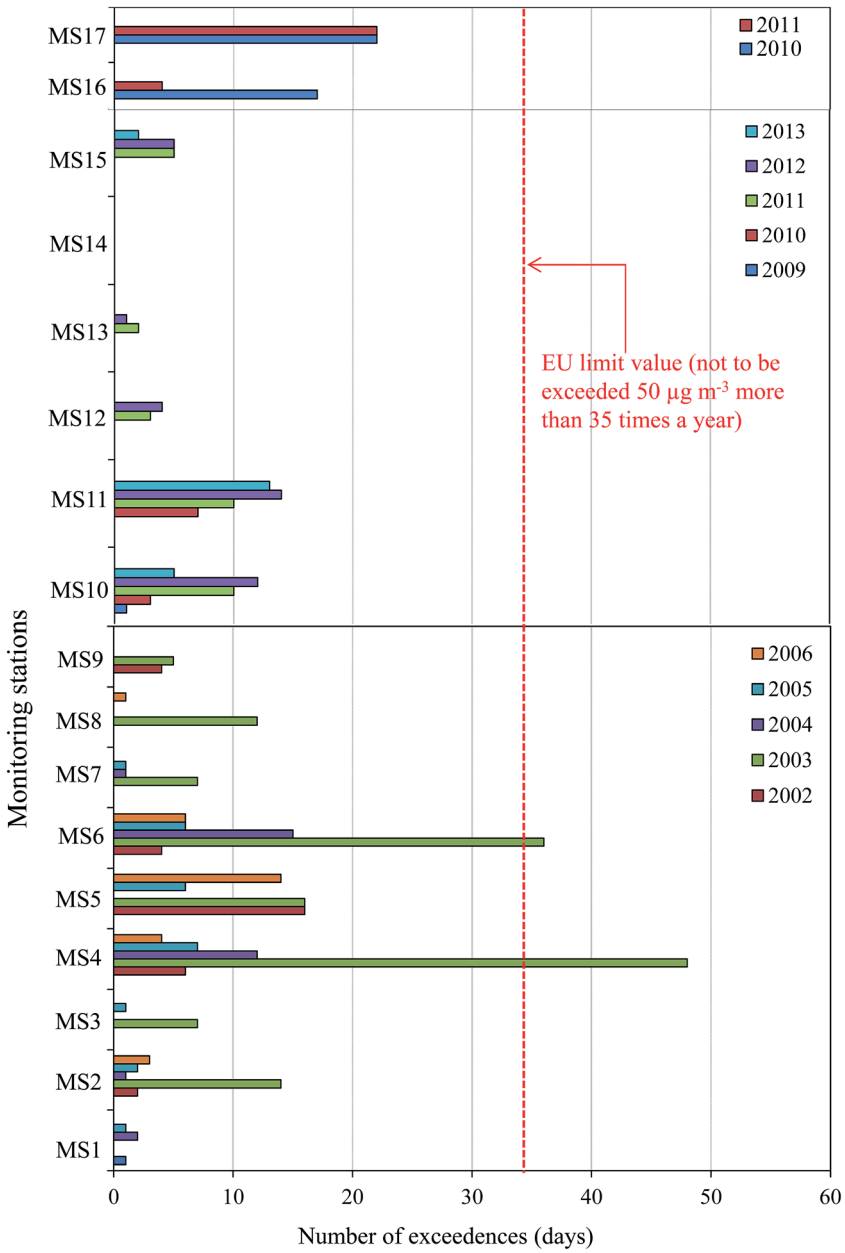

Fig. 8 The number of exceedences over the EU limit value at the individual monitoring stations. It should be noted that the exceedences presented in the figure are those based on the 24 h average limit values using the non-reference instruments for the durations when wind was blowing from construction sites towards the monitoring stations.

Furthermore, the calculated concentrations for PM_{10} and $PM_{2.5}$ were filtered on the basis of prevailing wind direction.

The decay profile of the PM_{10} concentrations at CS_1 was drawn using the data measured at MS_4, MS_5, MS_7 and MS_3, which were 100, 200, 500 and 1000 m away from CS_1, respectively. Moreover, the data measured at MS_4, MS_6 and MS_7 were used to draw the decay profile of $PM_{2.5}$ at CS_1, which were 100, 200 and 500 m away from CS_1, respectively. Furthermore, the decay profiles of the PM_{10} concentrations were measured at 100, 200 and 400 m away from CS_2 at MS_{10}, MS_{11} and MS_{15}, respectively.

Because of atmospheric dilution, the mass concentration dramatically decreased with an increasing distance from the construction site to approximately half of its value at a distance between 100 and 200 m. The best fitting logarithmic decay equations for PM_{10} were drawn, which gave R^2 values of 0.92 and 0.91 for CS_1 and CS_2, respectively (Fig. 9a). A much higher rate of change in the PM concentrations can be observed close to the construction site when compared with those at greater distances. For instance, the rate of change in PM_{10} (CS_1) concentration with per meter distance was 0.06 μg m^{-3} in between 100 and 200 m, which decreases to 0.030 and 0.013 μg m^{-3} per meter distance in the 200–400 m and 400–1000 m range, respectively (Fig. 9a). These observations suggest to measure the PM within a few 100 meters distance from the construction sites to capture the rapid decay in PMCs. The total

 This journal is © The Royal Society of Chemistry 2016

Open Access Article. Published on 07 dezembro 2015. Downloaded on 17/11/2024 04:07:55.
This article is licensed under a Creative Commons Attribution 3.0 Unported Licence.

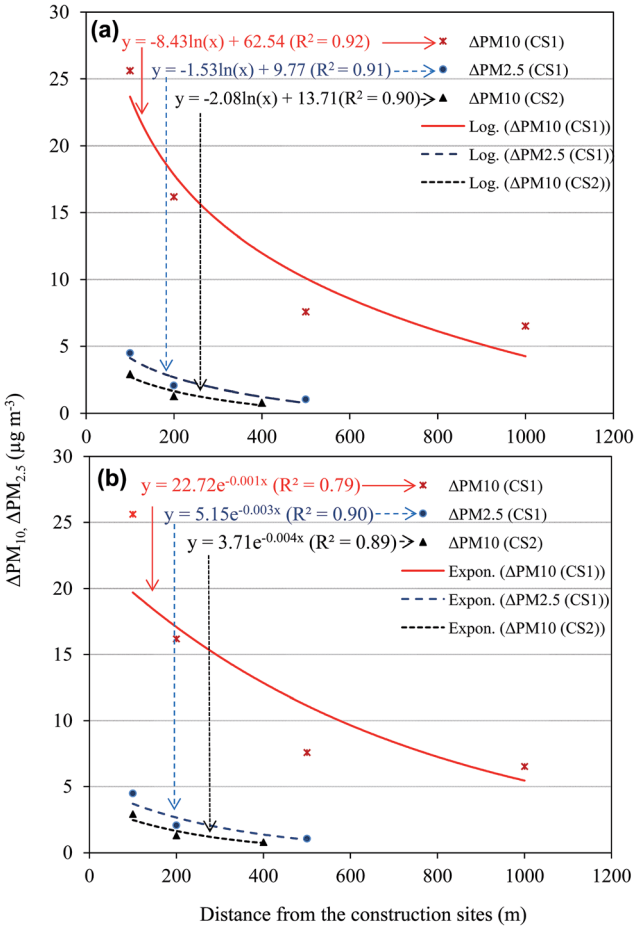

Fig. 9 ΔPM_{10} and $\Delta PM_{2.5}$ concentration decay at CS_1 and CS_2 *versus* the distance in the direction of wind blowing from the construction sites showing the (a) logarithmic and (b) exponential best fit functions. In the fitting equations, *x* and *y* express the distance from principal construction site and the PM_{10} values, respectively. The solid lines represent the best fitting decay curves.

mean $PM_{2.5}$ levels around CS_1 were also correlated well with the distances. A logarithmic decay profile with R^2 value of 0.90 represented the measured data very well.

Although studies measuring the decay of the PM concentrations around the construction sites are rare, we tried to compare our data with the most relevant studies. For example, Hitchins *et al.*[63] determined the PM_{10} concentration at increasing distances from a road at two sites in Australia. They found that $PM_{2.5}$ and ultrafine particles decayed by up to half of their maximum initial concentrations within a distance of 100–150 m from the road. Likewise, Buonanno *et al.*[64] found the PM_{10} concentration values to decrease exponentially away from the freeway in Italy during weekly traffic conditions.

4. Summary and conclusions

OSIRIS (model 2315) and TEOM 1400 were used to measure the mass concentration of particles in the 0.1–10 μm size range around three construction sites at 17 monitoring stations over a period of 12 years between January 2002 and December 2013. The objectives were to understand the emission characteristics of coarse and fine particles from construction activities, identifying their contribution to the ambient levels of PM concentrations in the vicinity of these sites and their spatial decay away from the construction sites.

The following conclusions are drawn from this study:

The source characteristics of PM_{10} and $PM_{2.5}$ were investigated using bivariate concentration polar plots and *k*-means clustering techniques. The high concentrations of PM_{10} and $PM_{2.5}$ were observed at the paired monitoring stations during the construction works when the winds were blowing from construction sites towards the monitoring stations. A *k*-means clustering technique provided a useful development to the bivariate polar plots to assess the contribution of construction and other local sources.

Three clusters (5, 6 and 7) from a total of the 8 selected clusters showed strong evidence of a downward increase in PM_{10} and $PM_{2.5}$ levels during the weekdays. These clusters were identified to represent construction activities.

PM_{10} were found about ~24%, 18% and 120%, and $PM_{2.5}$ about 11%, larger during the working periods when compared with those during non-working periods at CS_1, CS_2 and CS_3, respectively. These increases were attributed to the construction works as indicated by the bivariate concentration polar plots and *k*-means clustering analysis. In addition, the downwind concentrations of PM_{10} were found to be relatively more influenced by construction works at CS_1 than the $PM_{2.5}$ concentrations.

The 24 h mean EU limit of value of 50 μg m^{-3} set by EU Directives for PM_{10} not to be exceeded more than 35 times a calendar year was breached on two occasions due to construction operations on downwind monitoring stations during the measurements taken between 2002 and 2013.

Both the total PM_{10} and $PM_{2.5}$ values during working periods in the downwind direction were found to be well correlated with distance with R^2 values over 0.90 in a logarithmic form. These concentrations reduced to half of their initial concentrations within a few 100 meters. This indicates that placing a monitoring station around a site within this peripheral distance could help capture the rapid decay of particles escaping from the construction sites.

The results presented in this study highlight the contributions of PM_{10} and $PM_{2.5}$ from construction works. The increase in the concentrations of PM_{10} and $PM_{2.5}$ at the downwind monitoring stations suggest that there is a need to design more detailed and appropriate risk mitigation strategies to limit the exposure to onsite workers and people that live in the surrounding environment. Further studies covering chemical fingerprinting of size fractionated PM from construction operations are recommended to understand their chemical composition as well as apportioning construction dust (*e.g.* using calcium and other similar minerals as a marker) from the exhaust emissions of construction machinery (*e.g.* using black carbon as a marker[65]), together with allowing to differentiate between the properties of construction dust and the PM produced by the most common source (*i.e.* road vehicles) in urban environments.[16,66]

Acknowledgements

The authorswould like to thank the University of the Surrey and Cara for supporting this study. The authors would like to thank the anonymous reviewers for their time to read the manuscript. We would like to thank the construction site managers for permitting the use of their measurements.

Open Access Article. Published on 07 dezembro 2015. Downloaded on 17/11/2024 04:07:55.
This article is licensed under a Creative Commons Attribution 3.0 Unported Licence.

References

1 M. R. Heal, P. Kumar and R. M. Harrison, *Chem. Soc. Rev.*, 2012, **41**, 6606–6630.
2 A. F. Davila, D. Rey, K. Mohamed, B. Rubio and A. P. Guerra, *Environ. Sci. Technol.*, 2006, **40**, 3922–3928.
3 H. R. Anderson, *Atmos. Environ.*, 2009, **43**, 142–152.
4 D. Loomis, *Epidemiology*, 2000, **11**, 2.
5 B. Brunekreef and S. T. Holgate, *Lancet*, 2002, **360**, 1233–1242.
6 C. A. Pope, *J. Aerosol Med.*, 2000, **13**, 335–354.
7 A. Chaloulakou, P. Kassomenos, N. Spyrellis, P. Demokritou and P. Koutrakis, *Atmos. Environ.*, 2003, **37**, 649–660.
8 J. Pekkanen, K. L. Timonen, J. Ruuskanen, A. Reponen and A. Mirme, *Environ. Res.*, 1997, **74**, 24–33.
9 S. S. Lim, T. Vos, A. D. Flaxman, G. Danaei, K. Shibuya, H. Adair-Rohani, M. A. AlMazroa, M. Amann, H. R. Anderson and K. G. Andrews, *Lancet*, 2013, **380**, 2224–2260.
10 G. Oberdörster, *Int. Arch. Occup. Environ. Health*, 2000, **74**, 1–8.
11 F. Amato, M. Pandolfi, A. Escrig, X. Querol, A. Alastuey, J. Pey, N. Perez and P. K. Hopke, *Atmos. Environ.*, 2009, **43**, 2770–2780.
12 G. W. Fuller, D. C. Carslaw and H. W. Lodge, *Atmos. Environ.*, 2002, **36**, 1431–1441.
13 G. W. Fuller and D. Green, *Atmos. Environ.*, 2004, **38**, 4993–5002.
14 K. Ho, S. Lee, J. C. Chow and J. G. Watson, *Atmos. Environ.*, 2003, **37**, 1023–1032.
15 G. Tian, S. Fan, G. Li and J. Qin, *Huanjing Kexue*, 2007, **28**, 2626–2629.
16 P. Kumar, A. Robins, S. Vardoulakis and R. Britter, *Atmos. Environ.*, 2010, **44**, 5035–5052.
17 P. Kumar, A. Robins, S. Vardoulakis and P. Quincey, *Particulogy*, 2011, **9**, 566–571.
18 M. Abu-Allaban, J. Gillies, A. Gertler, R. Clayton and D. Proffitt, *Environ. Monit. Assess.*, 2007, **132**, 155–163.
19 S. H. Cadle, P. A. Mulawa, E. C. Hunsanger, K. Nelson, R. A. Ragazzi, R. Barrett, G. L. Gallagher, D. R. Lawson, K. T. Knapp and R. Snow, *Environ. Sci. Technol.*, 1999, **33**, 2328–2339.
20 A. J. Kean, R. F. Sawyer and R. A. Harley, *J. Air Waste Manage. Assoc.*, 2000, **50**, 1929–1939.
21 J. C. Chow, J. G. Watson, J. L. Mauderly, D. L. Costa, R. E. Wyzga, S. Vedal, G. M. Hidy, S. L. Altshuler, D. Marrack and J. M. Heuss, *J. Air Waste Manage. Assoc.*, 2006, **56**, 1368–1380.
22 M. Dall'Osto, A. Thorpe, D. Beddows, R. Harrison, J. Barlow, T. Dunbar, P. Williams and H. Coe, *Atmos. Chem. Phys.*, 2011, **11**, 6623–6637.
23 P. K. Hopke, R. E. Lamb and D. F. S. Natusch, *Environ. Sci. Technol.*, 1980, **14**, 164–172.
24 P. Kumar and L. Morawska, *Atmos. Environ.*, 2014, **90**, 51–58.
25 P. Kumar, L. Pirjola, M. Ketzel and R. M. Harrison, *Atmos. Environ.*, 2013, **67**, 252–277.
26 N. Saliba, F. El Jam, G. El Tayar, W. Obeid and M. Roumie, *Atmos. Res.*, 2010, **97**, 106–114.
27 G. E. Andrews, I. D. Andrews, D. W. Dixon-Hardy, B. M. Gibbs, H. Li and S. Wright, *ASME Turbo Expo 2010: Power for Land, Sea, and Air*, American Society of Mechanical Engineers, 2010, pp. 363–375.
28 J. J. Corbett, J. J. Winebrake, E. H. Green, P. Kasibhatla, V. Eyring and A. Lauer, *Environ. Sci. Technol.*, 2007, **41**, 8512–8518.
29 T. S. Bates, P. K. Quinn, D. Coffman, K. Schulz, D. S. Covert, J. E. Johnson, E. J. Williams, B. M. Lerner, W. M. Angevine, S. C. Tucker, W. A. Brewer and A. Stohl, *J. Geophys. Res.: Atmos.*, 2008, **113**, D00F01.
30 B. M. Barratt and G. W. Fuller, *Environ. Sci.: Processes Impacts*, 2014, **16**, 1328–1337.
31 D. Hansen, B. Blahout, D. Benner and W. Popp, *J. Hosp. Infect.*, 2008, **70**, 259–264.
32 C. M. Beck, A. Geyh, A. Srinivasan, P. N. Breysse, P. A. Eggleston and T. J. Buckley, *J. Air Waste Manage. Assoc.*, 2003, **53**, 1256–1264.
33 S. Dorevitch, H. Demirtas, V. W. Perksy, S. Erdal, L. Conroy, T. Schoonover and P. A. Scheff, *J. Air Waste Manage. Assoc.*, 2006, **56**, 1022–1032.
34 J. Joseph, R. S. Patil and S. K. Gupta, *Environ. Monit. Assess.*, 2009, **159**, 85–98.
35 S. Upton, *Effects of a construction site on local PM_{10} levels*, presentation at the Investigation of Air Pollution Standing Conference, Manchester, June 2002.
36 G. E. Muleski, C. Cowherd and J. S. Kinsey, *J. Air Waste Manage. Assoc.*, 2005, **55**, 772–783.
37 C. O. Egbu, *Construction Management and Economics*, 1999, **17**, 29–43.
38 A. Kousa, J. Kukkonen, A. Karppinen, P. Aarnio and T. Koskentalo, *Atmos. Environ.*, 2002, **36**, 2109–2119.
39 P. J. Lioy, C. P. Weisel, J. R. Millette, S. Eisenreich, D. Vallero, J. Offenberg, B. Buckley, B. Turpin, M. Zhong and M. D. Cohen, *Environ. Health Perspect.*, 2002, **110**, 703.
40 M. Abu-Allaban, S. Hamasha and A. Gertler, *J. Air Waste Manage. Assoc.*, 2006, **56**, 1440–1444.
41 E. U. Directive, *Off. J. Eur. Communities: Legis.*, 1999, **50**, 41–60.
42 E. U. Directive, *Off. J. Eur. Communities: Legis.*, 2008, **151**, 1–44.
43 D. C. Carslaw and K. Ropkins, *Environ. Model. Software*, 2012, **27–28**, 52–61.
44 J. Cyrys, G. Dietrich, W. Kreyling, T. Tuch and J. Heinrich, *Sci. Total Environ.*, 2001, **278**, 191–197.
45 F. Defra, TG, 09, 2009.

 This journal is © The Royal Society of Chemistry 2016

Open Access Article. Published on 07 dezembro 2015. Downloaded on 17/11/2024 04:07:55.
This article is licensed under a Creative Commons Attribution 3.0 Unported Licence.

46 D. C. Green, G. W. Fuller and T. Baker, *Atmos. Environ.*, 2009, **43**, 2132–2141.
47 G. P. Ayers, M. D. Keywood and J. L. Gras, *Atmos. Environ.*, 1999, **33**, 3717–3721.
48 M. B. Meyer, H. Patashnick, J. L. Ambs and E. Rupprecht, *J. Air Waste Manage. Assoc.*, 2000, **50**, 1345–1349.
49 D. Green, G. Fuller and B. Barratt, *Atmos. Environ.*, 2001, **35**, 2589–2593.
50 V. Tasić, M. Jovašević-Stojanović, S. Vardoulakis, N. Milošević, R. Kovačević and J. Petrović, *Atmos. Environ.*, 2012, **54**, 358–364.
51 K. Y. Kim, Y. S. Kim, Y. M. Roh, C. M. Lee and C. N. Kim, *J. Hazard. Mater.*, 2008, **154**, 440–443.
52 J. Gulliver and D. Briggs, *Atmos. Environ.*, 2004, **38**, 1–8.
53 D. C. Carslaw and S. D. Beevers, *Environ. Model. Software*, 2013, **40**, 325–329.
54 H. E. Smethurst, C. Witham, A. G. Robins and V. S. G. Murray, *J. Wind Eng. Ind. Aerod.*, 2012, **103**, 60–72.
55 Y.-J. Liu and R. M. Harrison, *Atmos. Environ.*, 2011, **45**, 3267–3276.
56 A. M. Jones, R. M. Harrison and J. Baker, *Atmos. Environ.*, 2010, **44**, 1682–1690.
57 A. Font, T. Baker, I. S. Mudway, E. Purdie, C. Dunster and G. W. Fuller, *Sci. Total Environ.*, 2014, **497–498**, 123–132.
58 B. Everitt, S. Landau, M. Leese and D. Stahl, *Cluster Analysis Wiley Series in Probability and Statistics*, Wiley, Chichester, UK, 2011, 5th edn, p. 346.
59 S. Wood, *Generalized additive models: an introduction with R*, CRC press, 2006.
60 M. A. Elangasinghe, N. Singhal, K. N. Dirks, J. A. Salmond and S. Samarasinghe, *Atmos. Environ.*, 2014, **94**, 106–116.
61 G. Jenkins, M. Perry and J. Prior, *The climate of the United Kingdom and recent trends*, Met Office Hadley Centre, Exeter, UK, 2009.
62 P. Kumar, M. Mulheron and C. Som, *J. Nanopart. Res.*, 2012, **14**, 771, DOI: 10.1007/s11051-012-0771-2.
63 J. Hitchins, L. Morawska, R. Wolff and D. Gilbert, *Atmos. Environ.*, 2000, **34**, 51–59.
64 G. Buonanno, A. Lall and L. Stabile, *Atmos. Environ.*, 2009, **43**, 1100–1105.
65 M. Viana, T. Kuhlbusch, X. Querol, A. Alastuey, R. Harrison, P. Hopke, W. Winiwarter, M. Vallius, S. Szidat and A. Prevot, *J. Aerosol Sci.*, 2008, **39**, 827–849.
66 P. Kumar, M. Ketzel, S. Vardoulakis, L. Pirjola and R. Britter, *J. Aerosol Sci.*, 2011, **42**, 580–603.